PHYSICAL REVIEW A VOLUME 46, NUMBER 10 15 NOVEMBER 1992

Hydrodynamic dispersion relations in dense fluids

Shankar P. Das and James W. Dufty
Department of Physics, University of Florida, Gainesville, Florida 32611
(Received 15 November 1991; revised manuscript received 14 May 1992)

Concepts of hydrodynamics and hydrodynamic modes are explored for dense fluids under conditions for which mode-coupling effects are important. Dispersion relations associated with the matrix of equilibrium time correlation functions for conserved densities are studied to isolate the hydrodynamic part of its spectrum. An Enskog-like model for hard spheres, including lowest-order bilinear density mode-coupling effects, is used for the analysis over a wide range of dense fluid conditions and for wavelengths extending down to those of the order of the correlation length. The hydrodynamic branch is identified as that which vanishes in the long-wavelength limit. The dispersion relations are investigated to determine the existence of such a hydrodynamic spectrum, and its possible extension to short wavelengths. Mode-coupling effects are shown to complicate the usual simple pole structure by introducing branch points that also vanish in the long-wavelength limit. Emphasis of this study is placed on the mode corresponding to heat diffusion. It is found that mode-coupling effects introduce significant changes in the extended modes, but the soft heat mode at wavelengths of the order of the correlation length remains a simple pole and provides the dominant contribution to the density autocorrelation function.

PACS number(s): 47.35.+i, 05.20.−y, 05.60.+w

I. INTRODUCTION

Understanding the microscopic origins of hydrodynamics is one of the most fundamental problems in nonequilibrium statistical mechanics [1]. Many years ago it was stressed by Onsager [2], Kadanoff and Martin [3], and McLennan [4] that the existence of hydrodynamics requires a very special analytic structure of equilibrium time correlation functions. In essence, the spectrum of correlation functions for local conserved densities must have isolated simple poles depending on the wave vector, k, which vanish as k goes to zero. Physically, the existence of poles which vanish for spatially homogeneous conditions simply expresses the existence of global conservation laws; the additional requirement of isolation at small wave vectors is sufficient (but not necessary) to explain why hydrodynamics dominates over excitations associated with other parts of the spectrum. Typically the latter are bounded away from zero by a value of the order of the collision frequency, so that for sufficiently small k the hydrodynamic pole is isolated and dominates the long-time behavior. In the intervening years, there have been two remarkable developments that suggest a closer look at this structure and its interpretation is required. These are (1) an extension of the hydrodynamic spectrum to large wave vectors (phenomena with wavelengths of the order of the correlation length or atomic dimension) [5], but still providing the dominant time dependence; and (2) the discovery of mode-coupling effects [6] that introduce a nonanalytic wave-vector dependence of the extended modes [7] and branch-point singularities that also move towards zero as k goes to zero, so that the hydrodynamic poles are not isolated [8]. The extended mode studies have been based on Enskog kinetic models which neglect mode-coupling effects, while mode-coupling effects on hydrodynamics have been limited to long wavelengths. As yet there has been no study of the nature of hydrodynamics, or even its existence, when both effects are considered. The objective here is to fill this gap with a detailed analysis of the hydrodynamic spectrum for a simple but realistic model defined for all wave vectors and including lowest-order mode-coupling effects. The clarification of hydrodynamics in this most general context is particularly relevant now because of its role in current descriptions of dense liquids. First, it has been shown that the concept of extended hydrodynamic modes is very useful in the analysis and interpretation of neutron scattering from simple dense liquids—a surprisingly simple picture of an otherwise complex many-body system has been obtained in this way [9]. Second, mode-coupling effects are at least part of the ingredients required for quantitative accuracy as the density is increased towards freezing [10]. Third, the coupling of extended modes provides both a qualitative and semiquantitative understanding of anomalous slow relaxation in dense equilibrium and metastable states observed in computer simulations [11,12]. We make some remarks on related but quite distinct studies of an ideal glass transition in the last section.

The simplest and most familiar concept of hydrodynamic modes is associated with the linearized Navier-Stokes equations. These are five coupled partial differential equations for the local conserved densities (mass, energy, and momentum), under conditions of small deviations from equilibrium. Harmonic solutions of the form $\exp\{i\omega t+i\mathbf{k}\cdot\mathbf{r}\}$ exist only if the angular frequency, ω, has a special relationship to the wave vector, $\mathbf{k}$. The special relationships, $\omega=\omega_\mu(k)$ (for $\mu=1,\ldots,5$) constitute the Navier-Stokes dispersion relations and completely characterize those equations. They have the form $\omega_1(k)=-\omega_2^*(k)=-ck+i\Gamma k^2$, $\omega_3(k)=iD_T k^2$, $\omega_4(k)$

$=\omega_5(k)=i\nu k^2$. The first two relations represent sound waves with velocity $\pm c\hat{\mathbf{k}}$ and damping constant Γ; the remaining three represent thermal and shear diffusion (the latter being being twofold degenerate) where D_T is the thermal diffusion coefficient and ν is the kinematic viscosity. The magnitude of the wave vector defines an associated wavelength, l, for the phenomena considered through, $k \equiv 2\pi/l$. Since the Navier-Stokes equations are valid only for wavelengths very large compared to the mean free path, l_0, the above expressions for $\omega_\mu(k)$ should be understood as the small-k form of more general dispersion relations applicable outside the Navier-Stokes limit. Extensions of these general dispersion relations to larger k *define* the "hydrodynamic" dispersion relations, continuously connected to the Navier-Stokes form in the small-k limit, that we wish to study here. We emphasize that our use of the terminology "hydrodynamics" below should be understood in this more general context, and is to be equated with Navier-Stokes hydrodynamics only in the small-k limit.

The dynamics of a simple fluid has "microscopic" as well as hydrodynamic dispersion relations. The hydrodynamic dispersion relations are distinguished by the property $\omega_\mu(k=0)=0$, reflecting the fact that the local conserved densities become global conserved quantities in this limit. This property is responsible for the dominance of hydrodynamic excitations at long times: As the system approaches equilibrium, characteristic wavelengths increase and the decay times for the hydrodynamic excitations increase while microscopic excitations approach a constant value of the order of the mean free time, t_0. This separation of time scales, $t_0 \ll \omega_\mu^{-1}$, suggests a rapid (exponentially fast) relaxation to a time scale on which the Navier-Stokes hydrodynamical description dominates.

The above qualitative description of hydrodynamics is supported in detail for low-density gases by calculations based on the Boltzmann equation [1,13]. Extended hydrodynamic modes based on the Boltzmann equation have been studied near the Navier-Stokes limit, leading to Burnett and super-Burnett order hydrodynamics [1]. When mode-coupling effects are included at low density the Burnett order transport coefficients are found to diverge, indicating a nonanalytic dependence on the wave vector. In addition, there are branch points at $\omega \sim k^2$ which lead to additional dynamics on the same time scale as the Navier-Stokes hydrodynamic modes. These mode-coupling effects on lowest-order small-k corrections to Navier-Stokes modes have been studied in some detail [7,8]. However, a neccesary condition for hydrodynamics is that the wave vector be small compared to the mean free path. At low density this restricts attention to the small-k domain for which both the nonanalytic corrections and branch-point effects are small. Thus the low-density calculations clearly signal qualitative changes in hydrodynamics beyond Navier-Stokes order due to mode coupling, but without a significant quantitative effect.

The circumstances at high density are quite different for two reasons. First, the mean free path becomes smaller than the atomic dimension so the potential domain of hydrodynamics extends to much larger k values. Second, the amplitude of the mode-coupling contribution increases significantly with density. The dense fluid (near freezing) is therefore precisely the system for which the concept of extended modes becomes relevant, but also that for which mode-coupling effects must be included. It is important to clarify at this point why a study of the extended hydrodynamic modes, among all the other excitations that can occur at such short wavelengths, is significant at all. Indeed, it might appear at first that the extended hydrodynamic modes (if they should exist) simply provide one of many small contributions to the dynamics on a given time scale, and therefore are of little interest. Surprisingly, however, the extended hydrodynamic modes still appear to give the dominant contribution to the dynamics [5]. There are two reasons for this. First, sum rules for the correlation functions impose a relationship between the amplitudes of the microscopic and hydrodynamic modes such that the former are small compared to the latter, as long as the hydrodynamic poles, $\omega_\mu(k)$, are smaller than the microscopic singularities [14]. Second, the extension of the Navier-Stokes heat mode "softens" (becomes very small) at wave vectors of the order of the inverse atomic size (an enhancement of de Gennes narrowing) [5]. The combination of these two phenomena allows the correlation functions to be calculated quantitatively from the heat mode alone. It is truly a remarkable result that the dynamical properties of a dense, strongly coupled, many-body system can be given over a wide range of space, time, and density parameters can be explained in terms of a few dominant excitations. This is the primary motivation for the study of extended hydrodynamics, its existence under more general conditions, and its limitations. Our objective here is to explore the hydrodynamic spectrum under the more general conditions of both large wave vectors and mode-coupling effects, with particular attention to the hydrodynamic branch corresponding to the heat mode and its softening at the correlation length.

In the next section, the relationship of hydrodynamics to equilibrium time correlation functions is noted, and the nature of the problem is illustrated for the simpler case of self-diffusion. The origin of both mode-coupling and short-wavelength effects is discussed and illustrated. As indicated above, the combined effects become quantitatively significant only at higher densities. The description of dynamics at high densities over a wide range of wave vectors is a formidable problem for which a controlled and accurate theoretical description is not yet available. We consider here a phenomenological model for the hard-sphere fluid that has all the relevant qualitative effects and is semiquantitative even at high densities. The details of this model are described and discussed in Sec. III and the Appendix. The hydrodynamic dispersion relations are identified for this model first with mode-coupling effects neglected. The characteristic features of the k dependence of $\omega_\mu(k)$ beyond the Navier-Stokes limit is discussed for high densities. The set $\{\omega_\mu(k)\}$ in this approximation represent simple poles in the analytic structure of the correlation function matrix, whose location varies with wave vector. In particular, the soft-heat mode mentioned above is identified.

The additional effects of mode coupling are considered next. New singular points appear, branch points, that modify significantly the dynamics at intermediate wave vectors. The modifications of the sound and heat mode branches are studied over a wide range of wave vectors. At wave vectors of the order of the inverse correlation length, the soft-heat mode is further softened relative to the Enskog value, and the singularity appears to remain a simple pole. At somewhat smaller, but still intermediate, wave vectors the singularity becomes a branch point with a wave-vector-dependent exponent.

The model considered here also can be solved exactly, without the necessity to identify separately contributions from different types of singularities. This is done in Sec. VI. The exact density autocorrelation function for the model is compared to the contribution from the hydrodynamic singularities alone. In the domain of wave vectors near the inverse correlation length, the soft-heat mode is found to provide the dominant contribution to the correlation function for all but the shortest times. Thus the nature of the extended modes based on the simple Enskog model (neglecting mode coupling) is justified for this domain. At shorter wave vectors where the simple pole structure no longer applies, it appears that several singularities contribute to the correlation function in addition to the heat mode. The results are summarized and discussed in the last section.

II. TIME CORRELATION FUNCTIONS AND HYDRODYNAMICS

The relationship between equilibrium time correlation functions and linear hydrodynamics was noted in the classic papers of Onsager in 1931 [2], and formalized in more detail by many others [3,4]. In summary, it is possible to show that the response to small initial perturbations from an equilibrium state is governed by the equilibrium time correlation functions for the local conserved densities. Consequently, all excitations (including hydrodynamics, when it exists) can be determined from a study of the dynamics of these correlation functions. The response to an excitation of wavelength, l, is determined by the correlation functions for the conserved densities with Fourier components of magnitude $k=2\pi/l$,

$$C_{\alpha\beta}(k,t)=\langle a_\alpha(\mathbf{k},t)[a_\beta^*(\mathbf{k},0)-\langle a_\beta^*(k)\rangle]\rangle \ . \tag{2.1}$$

The brackets denote an equilibrium ensemble average and the microscopic conserved densities in Fourier representation are

$$a_\alpha(\mathbf{k})\leftrightarrow(\rho(\mathbf{k}),\varepsilon(\mathbf{k}),\hat{\mathbf{k}}\cdot\mathbf{g}(\mathbf{k}),\hat{\mathbf{e}}_1\cdot\mathbf{g}(\mathbf{k}),\hat{\mathbf{e}}_2\cdot\mathbf{g}(\mathbf{k})) \ , \tag{2.2}$$

$$\rho(k)=V^{-1/2}\sum_i m\exp[i\mathbf{k}\cdot\mathbf{q}_i] \ , \tag{2.3}$$

$$\varepsilon(k)=V^{-1/2}\sum_i [\tfrac{1}{2}mv_i^2-\tfrac{3}{2}k_BT]\exp[i\mathbf{k}\cdot\mathbf{q}_i] \ , \tag{2.4}$$

$$\mathbf{g}(\mathbf{k})=V^{-1/2}\sum_i m\mathbf{v}_i\exp[i\mathbf{k}\cdot\mathbf{q}_i] \ , \tag{2.5}$$

where ρ, ε, and $\mathbf{g}$ are the mass, energy, and momentum densities, respectively. The coordinate and velocity of the ith particle are denoted by $\{\mathbf{q}_i,\mathbf{v}_i\}$, m is the mass, T is the temperature, and V is the volume of the system. Only the kinetic part of the energy occurs since attention ultimately will be restricted to hard spheres. Also, $\hat{\mathbf{e}}_1$ and $\hat{\mathbf{e}}_2$ are unit vectors orthogonal to $\mathbf{k}$ and characterize the transverse momentum density components.

The Laplace transform of this correlation matrix is defined by

$$\tilde{C}_{\alpha\beta}(\mathbf{k},z)=\int_0^\infty dt\, e^{-zt}C_{\alpha\beta}(\mathbf{k},t) \ . \tag{2.6}$$

Stationarity of the equilibrium average implies the inequality

$$|C_{\alpha\beta}(\mathbf{k},t)|\le[C_{\alpha\alpha}(\mathbf{k},0)C_{\beta\beta}(\mathbf{k},0)]^{1/2} \ . \tag{2.7}$$

It follows that the matrix elements $\tilde{C}_{\alpha\beta}(\mathbf{k},z)$ are analytic in the half plane, $\mathrm{Re}z>0$. The inverse transform can be given by

$$C_{\alpha\beta}(\mathbf{k},t)=(2\pi i)^{-1}\int_{-i\infty}^{i\infty}dz\, e^{zt}\tilde{C}_{\alpha\beta}(\mathbf{k},z) \ . \tag{2.8}$$

The singular points (poles, branch points, essential singularities) of $\tilde{C}_{\alpha\beta}(\mathbf{k},z)$ in the half plane $\mathrm{Re}z\le0$ completely characterize the time-dependent response of the fluid to any small initial pertubation. To help identify the analytic structure of $\tilde{C}_{\alpha\beta}(\mathbf{k},z)$ it is useful to define an associated transport matrix, $M_{\alpha\beta}(k,z)$, by

$$\tilde{C}(\mathbf{k},z)=[z+M(k,z)]^{-1}C(k) \ . \tag{2.9}$$

An obvious matrix notation has been introduced in the last equation, and $C(\mathbf{k})=C(\mathbf{k},t=0)$ is the equal time correlation function matrix. The general dispersion relations, $z=z_\mu(k)$, are now defined as the solutions to

$$\mathrm{Det}[z_\mu+M(k,z_\mu)]=0 \ . \tag{2.10}$$

Such solutions (both poles and branch points) contribute a time dependence $\sim\exp[z_\mu(k)t]$ with time scale $1/\mathrm{Re}z_\mu(k)$. The dependence of these solutions on k is the property of interest here and two classes of solutions are distinguished for the hydrodynamic "modes," and microscopic "modes," respectively:

$$\lim_{k\to0}z_\mu(k)=0 \ ,$$
$$\lim_{k\to0}z_\mu(k)\neq0 \ . \tag{2.11}$$

Equation (2.11) gives the precise meaning to "hydrodynamics" as distinguished from all other dynamics, and defined for all k such that solutions to (2.9) exist: Those whose dispersion relations are continuously connected to $k=0$. They need not represent simple poles, as in the Navier-Stokes case, and consequently do not necessarily lead to pure exponential decay in time. Also, it is possible to have a greater number of such solutions than the number of conserved densities. However, the amplitudes of the excess number of hydrodynamic modes should vanish as $k\to0$.

The Navier-Stokes form for the hydrodynamic modes is recovered in the limit $k\to0$ by noting that $M(k,z)$ has the exact form (see Appendix)

$$M(k,z)=ik\Omega(k)+k^2\Lambda(k,z) \tag{2.12}$$

so that the dispersion relations to order k^2 formally are determined from

$$\mathrm{Det}[z_\mu + ik\Omega(0) + k^2\Lambda(0,0) + O(k^3)] = 0 \ . \tag{2.13}$$

The matrix Ω determines the Euler level modes, and the eigenvalues of $\Lambda(0,0)$ yield the formal Green-Kubo expressions for Navier-Stokes order transport coefficients [15,16].

Before introducing our model for calculation of the matrix $M(k,z)$, the remainder of this section provides an illustration of the phenomena to be studied using self-diffusion at low density as an example. The results are based on calculations using the Boltzmann equation modified to include correlated "ring" collisions. The latter lead to the mode-coupling effects mentioned in the introduction. The relevant time correlation function in this case is

$$C(k,t) \equiv \langle \exp\{i\mathbf{k}\cdot[\mathbf{q}(t) - \mathbf{q}(0)]\} \rangle \ . \tag{2.14}$$

The matrix $M(k,z)$ can be calculated to first order in the ring collision amplitudes to determine the spectrum of the correlation function. There are two parts, that which vanishes as k goes to zero and that which remains finite in this limit. The correlation function can be written in terms of the corresponding hydrodynamic and microscopic parts, $\tilde{C}_h(\mathbf{k},z)$ and $\tilde{C}_m(\mathbf{k},z)$, respectively (only the results are quoted here; see Ref. [8] for details),

$$\tilde{C}(\mathbf{k},z) \equiv \int_{-\infty}^{\infty} dt\, e^{-zt} C(\mathbf{k},t) = \tilde{C}_h(\mathbf{k},z) + \tilde{C}_m(\mathbf{k},z) \ , \tag{2.15}$$

$$\tilde{C}_h(\mathbf{k},z) = [z + D(k,z)k^2]^{-1} \ , \tag{2.16}$$

$$\tilde{C}_m(\mathbf{k},z) = \beta m [D(k)k]^2 [z + \mu(k,z)]^{-1} \ , \tag{2.17}$$

$$D(k,z) = [\beta m \mu(k,z)]^{-1} \ , \tag{2.18}$$

$$\mu(k,z) = [1 - A(k,z)]/\beta m D(k) \ . \tag{2.19}$$

Here, $A(k,z)$ denotes the effects of mode coupling. If $A(k,z)$ is neglected, there are two simple poles in the spectrum, at $z = -D(k)k^2$ and $z = -1/\beta m D(k)$. The Laplace transform is inverted to give the correlation function in the approximation

$$C(k,t) = \exp[-D(k)k^2 t] + \beta m [D(k)k]^2 \exp[-t/\beta m D(k)] \ . \tag{2.20}$$

For small k, $D(k)$ approaches a constant $D(0)$, and the first term represents simple hydrodynamic diffusion. For larger k, $D(k)$ is analytic in k^2 and contains corrections to diffusion associated with Burnett and higher-order hydrodynamics [14]; $D(k)k^2$ is the extended hydrodynamic mode with characteristic time $t_h(k) = 1/D(k)k^2$. In contrast, the second term decays to zero for $t > t_m(k) \equiv \beta m D(k)$. Thus the first term will exponentially dominate the second for $t \gg t_m$, as long as $t_h(k) > t_m(k)$. These conditions are always valid at very small k, but also apply more generally for $kl_0 < 1$, where l_0 is the mean free path. Note also that the amplitude of the hydrodynamic part is larger than that of the microscopic part for $t_h(k) > t_m(k)$, as indicated in the introduction. It is shown in Ref. [14] that the hydrodynamic part dominates in this domain, and that this domain exists well beyond the small-k diffusive limit. While these results are not striking, they serve to illustrate the notion and relevance of an extended hydrodynamic mode.

Now consider the changes due to inclusion of mode-coupling effects. To simplfy the discussion only the small-k and -z form of $A(k,z)$ in (2.19) is considered,

$$A(k,z) = a(z_\mu + \alpha k^2)^{1/2} \ . \tag{2.21}$$

Here a is the amplitude of the mode-coupling term, and $\alpha = \nu D/(\nu + D)$ where ν is the kinematic viscosity and $D = D(0)$. The dispersion relations for the hydrodynamic part become

$$z_\mu = -Dk^2[1 - a(z_\mu + \alpha k^2)^{1/2}] \ . \tag{2.22}$$

The second term of the brackets leads to qualitative differences. First, note that since $z_\mu \sim k^2$ this term cannot be neglected for small k. There is a branch point at $-\alpha k^2$ and the associated branch cut is chosen along $\mathrm{Re}z \le -\alpha k^2$. Solutions to (2.22) are therefore restricted to $z_h \equiv Re^{i\theta}$ with $R \ge 0$ and $-\pi < \theta < \pi$. These solutions to leading order in k are found to be

$$z_\mu(k) = -Dk^2[1 \pm ia(D - \alpha)^{1/2}k] \ . \tag{2.23}$$

The term of order k^3 cannot be neglected, since it is the dominant imaginary part. Furthermore, if this term were neglected, the resulting singularity at $-Dk^2$ would be on the branch cut since $D > \alpha$. Instead of one hydrodynamic branch, there are now necessarily two branches: Navier-Stokes order hydrodynamics has been changed from one diffusive mode to two propagating modes by the mode-coupling effects. The time dependence of the correlation function has a hydrodynamic part arising from three singular points, all of which vanish as $k \to 0$: the branch point at $-\alpha k^2$ and the two simple solutions (2.23). Closer inspection shows the latter two are simple poles. Inverting the Laplace transform then gives

$$C_h(k,t) = e^{-Dk^2 t}[2\cos(\omega t) + kaD(D - \alpha)^{-1/2}\sin(\omega t)] - e^{-\alpha k^2 t} aDk^2 \pi^{-1} \int_0^\infty dx\, \sqrt{x}\, e^{-xt} \{(x - [D - \alpha]k^2)^2 + x(aDk^2)^2\}^{-1} \tag{2.24}$$

with $\omega = aD(D - \alpha)k^3$. The first two terms are due to the poles, while the last term is due to the branch point. The Navier-Stokes form is recovered only in the formal limit $k \to 0$ at constant $\tau \equiv Dk^2 t$.

The illustrations of the last two paragraphs indicate the nature of the problem addressed more generally in subsequent sections. The primary observations from the above are as follows. (1) Hydrodynamic modes exist for

wave vectors $kl_0 < 1$ although the form of the dispersion relation, $z_h(k)$, generally differs from the Navier-Stokes form except at very small k. (2) Mode-coupling effects at small k change the simple diffusive mode of the Navier-Stokes equations to two propagating modes; hydrodynamic modes still exist as simple poles but are qualitatively different. (3) Mode-coupling effects introduce additional singular points of $C(\tilde{k},z)$ (in this case a square-root branch point). (4) While the Navier-Stokes form is recovered in an asymptotic sense, it is no longer exponentially separated from the dynamics induced by the branch cut. (5) A similar analysis of the microscopic part $C_m(k,t)$ leads to a contribution from the branch cut that persists on the same time scale as hydrodynamics; however, the smaller amplitude still allows the hydrodynamic part to dominate.

These conditions suggest the following questions for exploration in the next sections: Do extended hydrodynamic modes exist and under what conditions? Are the modes simple poles or more complex singularities? Do the hydrodynamic singularities dominate those from branch cuts?

III. A MODEL FOR DENSE FLUID DYNAMICS

To describe more general processes involving transport of mass, energy, and momentum, we consider a simple, tractable model that retains the correct static structural features of dense fluids, yields reasonable transport coefficients, and describes the dominant mode-coupling effects. The model consists of an approximation to the transport matrix, $M(k,z)$, of Eq. (2.9). A convenient, formally exact, representation of this matrix is obtained in the Appendix. The high-frequency limit can be isolated to write

$$M(k,z)=M(k,z=\infty)+\Delta M(k,z) . \tag{3.1}$$

The first term on the right side describes the exact short-time dynamics of the correlation function matrix, and can be calculated explicitly. The results are given in the Appendix. It is a remarkable feature of the hard-sphere fluid that this term by itself is a good first approximation. It is not restricted with respect to wave vector or density, it yields semiquantitative values for all transport coefficients at high densities, and it gives a good representation of the hydrodynamic modes over all wave vectors (compared to those of Ref. [5] based on the Enskog kinetic theory) [17].

Consider next the evaluation of $\Delta M(k,z)$. The representation given in the Appendix shows it is block diagonal, with many zero elements resulting from fluid symmetries,

$$\Delta M=\begin{bmatrix} 0 & 0 & 0 & 0 & 0 \\ 0 & \Delta M_{22} & \Delta M_{23} & 0 & 0 \\ 0 & \Delta M_{32} & \Delta M_{33} & 0 & 0 \\ 0 & 0 & 0 & \Delta M_{44} & 0 \\ 0 & 0 & 0 & 0 & \Delta M_{55} \end{bmatrix} . \tag{3.2}$$

Furthermore, $\Delta M_{44}=\Delta M_{55}$. There are two types of contributions to ΔM. One is due to dynamical correlations that develop and then decay over times of the order of a few collision times; the other is due to dynamical correlations that take longer to develop and persist to much later times. To estimate the nonzero elements, these short- and long-time contributions are first separated according to

$$\Delta M(k,z)=\int_0^{\tau} dt\, e^{-zt}\Delta\mathcal{M}(k,t)+\int_{\tau}^{\infty} dt\, e^{-zt}\Delta\mathcal{M}(k,t) . \tag{3.3}$$

The persistent correlation effects of the second term are approximated here by a simple mode-coupling theory, described below, which applies (and dominates) only after a sufficiently long time, τ. The value of τ used here is obtained by fitting the integrand of (3.3) calculated from the mode-coupling theory to results from computer simulation [11,12], giving $\tau\sim 10\tau_e$. Here $\tau_e=\sigma\sqrt{\beta m\pi}/4\pi n^* g(\sigma)$ is the mean free time calculated from the Enskog kinetic theory, and $g(\sigma)$ is the radial distribution function at contact. This can only be considered as an estimate.

The first term on the right side of (3.3) represents short-time dynamics and can be estimated from the Enskog kinetic theory [10]. However, the dominant contribution to the total matrix, M, from the Enskog kinetic theory is already contained in the high-frequency part, $M(k,z=\infty)$. Furthermore, it has been shown recently [18] that this intermediate-time domain has significant contributions beyond those of the simple Enskog theory. In light of the uncertainties arising from the choice of τ, the complexity of the dynamics for $t<\tau$, and the relatively small magnitude of this contribution, it is reasonable to neglect entirely the first term on the right side of (3.3). This leads to an underestimate of the transport coefficients relative to the complete Enskog theory, although the qualitative density dependence is preserved at high density. In this approximation we have simply

$$\Delta M(k,z)=\int_{\tau}^{\infty} dt\, e^{-zt}\Delta\mathcal{M}^{\mathrm{MC}}(k,t) . \tag{3.4}$$

The superscript, MC, denotes the mode-coupling contribution.

The mode-coupling contribution contains correlations among all possible bilinear pairs of the conserved densities. However, at high densities and long times the contributions from products of two densities, $\rho(\mathbf{k})\rho(\mathbf{k}')$, dominate all others. This is due to the fact that their amplitudes are largest and the soft-heat mode which dominates at long times has the density as an approximate eigenvector. Our final approximation is therefore to retain only the mode-coupling contributions from density nonlinearities. It then follows that the only nonzero elements of ΔM are ΔM_{33} and $\Delta M_{44}=\Delta M_{55}$. Their detailed form is given below.

Some final comments on this sequence of approximations are in order. The problem addressed, transport in a dense fluid over a wide range of wave vectors, is a formidable theoretical problem with no quantitative description available at present. More complete descriptions, such as that of Ref. [10], include some of the effects

neglected here (Enskog theory plus all bilinear modes). Even so, the uncertainties of the model at intermediate times and high densities are large and it is not clear that more accurate results are obtained. In this context, we have chosen perhaps the simplest realistic model to discuss the qualitative features of hydrodynamic modes, albeit with only semiquantitative accuracy.

The shear modes are somewhat simpler to describe and therefore are considered first. The subspace (4,5) associated with transverse momentum density components is diagonal with $M_{44}=M_{55}$, and the dispersion relations become

$$z_4(k)+[\nu(k)+\nu^{\mathrm{MC}}(k,z_4)]k^2=0\ , \tag{3.5}$$

where $\nu(k)k^2\equiv M_{44}(k,z=\infty)$ is (from the Appendix)

$$\nu(k)k^2=\tfrac{2}{3}\tau_e^{-1}[1-3j_1(k\sigma)/(k\sigma)]\ . \tag{3.6}$$

Here $j_l(x)$ is the spherical Bessel function of order l, $\tau_e=\sigma\sqrt{\beta m\pi}/4\pi n^* g(\sigma)$ is the (Enskog) mean free time, and $g(\sigma)$ is the radial distribution function at contact. The mode-coupling contribution, $\nu^{\mathrm{MC}}(k)k^2$ is bilinear in the density correlation function, $C_{\rho\rho}(k,t)=C_{11}(k,t)$,

$$\nu^{\mathrm{MC}}(k,z)k^2=\int_\tau^\infty dt\, e^{-zt}\int d\mathbf{k}'\ A_1(\mathbf{k}',\mathbf{k}-\mathbf{k}')\times C_{\rho\rho}(k',t)C_{\rho\rho}(\mathbf{k}-\mathbf{k}',t)\ . \tag{3.7}$$

It is understood here that the correlation functions $C_{\rho\rho}$ in (3.4) are to be calculated in the approximation obtained by neglecting ΔM (lowest-order mode-coupling theory). The solution to (3.5) requires analytic continuation of (3.4) into the Re$z<0$ half plane.

Similar results are obtained for the longitudinal modes arising from the elements of M in the subspace (1,2,3). The contributions from $M(k,z=\infty)$ are given in the Appendix. The only nonvanishing mode-coupling effect appears in $M_{33}(k,z)$:

$$M_{33}(k,z)\equiv[\Gamma(k)+\Gamma^{\mathrm{MC}}(k,z)]k^2\ , \tag{3.8}$$

where $\Gamma(k)k^2\equiv M_{33}(k,z=\infty)$ is

$$\Gamma(k)k^2=\tfrac{2}{3}\tau_e^{-1}[1-3j_0(k\sigma)+6j_1(k\sigma)/(k\sigma)] \tag{3.9}$$

and $\Gamma^{\mathrm{MC}}(k,z)k^2$ is the bilinear density mode-coupling correction, with the same form as in (3.7) except with a different amplitude,

$$\Gamma^{\mathrm{MC}}(k,z)k^2=\int_\tau^\infty dt\, e^{-zt}\int d\mathbf{k}'\ A_2(\mathbf{k}',\mathbf{k}-\mathbf{k}')\times C_{\rho\rho}(k',t)C_{\rho\rho}(\mathbf{k}-\mathbf{k}',t)\ . \tag{3.10}$$

The hydrodynamic modes are now determined from (2.10), using the three-dimensional longitudinal submatrix of $M(k,z)$, to give

$$z_\mu^3+z_\mu^2[M_{22}(k)+M_{33}(k,z_\mu)]+z_\mu[M_{33}(k,z_\mu)M_{22}(k)-M_{32}(k)M_{23}(k)+M_{31}(k)M_{13}(k)]+[M_{31}(k)M_{13}(k)M_{22}(k)]=0\ , \tag{3.11}$$

where here and below we use the notation $M_{\alpha\beta}(k,\infty)\equiv M_{\alpha\beta}(k)$.

The mode-coupling effects are characterized by the two amplitudes, $A_1(\mathbf{k}',\mathbf{k}-\mathbf{k}')$ and $A_2(\mathbf{k}',\mathbf{k}-\mathbf{k}')$. These are expressed in terms of the two- and three-particle direct correlation functions, $c(k)$ and $c(\mathbf{k},\mathbf{k}')$, respectively,

$$A_1(\mathbf{k}',\mathbf{k}-\mathbf{k}')=\alpha[c(k')-c(\mathbf{k}-\mathbf{k}')]^2k'^2[1-(\hat{\mathbf{k}}\cdot\hat{\mathbf{k}}')]^2/2\ , \tag{3.12}$$

$$A_2(\mathbf{k}',\mathbf{k}-\mathbf{k}')=\alpha[\hat{\mathbf{k}}\cdot\hat{\mathbf{k}}'c(k')+\hat{\mathbf{k}}\cdot(\mathbf{k}-\mathbf{k}')c(\mathbf{k}-\mathbf{k}')+nc(\mathbf{k}',\mathbf{k}-\mathbf{k}')]^2\ , \tag{3.13}$$

where the constant $\alpha\equiv(2\pi)^{-3}(2\beta nm^5)^{-1}$. The only quantities required for calculations with the model are therefore the pair correlation function [or equivalently $c(k)$], and the three-particle correlation function $c(\mathbf{k},\mathbf{k}')$. The methods used for calculating these quantities are described in the next section.

IV. NAVIER-STOKES ORDER

To solve for the dispersion relations at small k (order k^2) it is sufficient to set $k=z=0$ in both $\nu^{\mathrm{MC}}(k,z)$ and $\Gamma^{\mathrm{MC}}(k,z)$, provided the latter exist. The dispersion relations are then the Navier-Stokes results (2.13), with transport coefficients defined by

$$\lambda=(3n\sigma^2k_B/10t_e)\left[1+\frac{2}{3}\frac{[1+4\bar{\eta}g(\sigma)]^2}{1-nc(0)}\right]\ ,$$
$$\Gamma=[\Gamma(k)+\Gamma^{\mathrm{MC}}(k,z)]_{k=z=0}\ , \tag{4.1}$$
$$\nu=[\nu(k)+\nu^{\mathrm{MC}}(k,z)]_{k=z=0}\ ,$$

where $\bar{\eta}=\pi n\sigma^3/6$ is the packing fraction. The thermal conductivity, λ, has no mode-coupling contribution in this model, and is given entirely by the contribution from $M(k)$. The Navier-Stokes dispersion relations obtained in this way apply only in the asymptotic limit described following (2.23); in general, a branch point arises from the mode-coupling terms in (4.1) and the dispersion relations give results with complex parts, similar to those from (2.23).

The mode-coupling contributions to Γ and ν are positive and therefore increase the viscosities over their Enskog values. To calculate the magnitude of these contributions it is first necessary to evaluate the two amplitudes, $A_1(\mathbf{k}',\mathbf{k}-\mathbf{k}')$ and $A_2(\mathbf{k}',\mathbf{k}-\mathbf{k}')$ of Eqs. (3.12) and (3.13), and the density autocorrelation function $C_{\rho\rho}(k,z)$ from (2.9) with $M\to M(k)$. Consider first the correlation function, which can be expanded in terms of the eigenvalues and eigenvectors of $M(k)$,

$$C_{\rho\rho}(k,t)/C_{\rho\rho}(k,0)\to\sum_{\mu=1}^{3}R_\mu(k)\exp[-\lambda_\mu(k)t]\,, \tag{4.2}$$

$$M(k)\phi_\mu(k)=\lambda_\mu(k)\phi_\mu(k)\,, \tag{4.3}$$

where $C_{\rho\rho}(k,0)=nm^2S(k)$, and $S(k)$ is the static structure factor. Expressions for the eigenvalues and residues $R_\mu(k)$ are given in the Appendix. The time integrals in Eqs. (3.7) and (3.10) now can be performed with the results

$$\nu=\nu^e+\int_0^1 dx\,\mathcal{A}_1(x)\mathcal{B}(x),\quad \Gamma=\Gamma^e+\int_0^1 dx\,\mathcal{A}_2(x)\mathcal{B}(x)\,, \tag{4.4}$$

$$\mathcal{A}_1(x)\equiv(60\pi^2\beta nm)^{-1}k_m^3\left[S(k_mx)x\frac{d}{dx}c(k_mx)\right]^2,$$

$$\mathcal{A}_2(x)\equiv(4\pi^2\beta nm)^{-1}k_m^3[S(k_mx)]^2\{[c(k_mx)+nc(k_mx,-k_mx)]^2+\tfrac{1}{5}[k_mxc(k_mx)]^2+\tfrac{2}{3}[c(k_mx)+nc(k_mx,-k_mx)]\}\,, \tag{4.5}$$

$$\mathcal{B}(x)=\sum_{\mu,\mu'}x^2R_\mu(k_mx)R_{\mu'}(k_mx)[\lambda_\mu(k)+\lambda_{\mu'}(k)]^{-1}\exp\{-\tau[\lambda_m(k)+\lambda_{\mu'}(k)]\}.$$

An upper limit of $k_m\sigma=25$ has been introduced in the k integration, representing a maximum value beyond which the modes do not exist (this is of similar magnitude to that found in Ref. [5]). As $C_{\rho\rho}(k,t)$ does not couple to the transverse modes, only the longitudinal modes appear.

The eigenvalues $\lambda_\mu(k)$ are the negative of the hydrodynamic modes associated with $M(k)$; their real and imaginary parts are shown in Figs. 1(a) and 1(b) for the density $n^*=0.9$. Of particular interest is the softening of the heat mode, $z_3(k)$ near the peak of $S(k)$ at $k\sigma\sim 6$. Figure 2 shows how this softening increases as a function of density. This shows that $C_{\rho\rho}(k,t)$ will have slowly decaying components both at small k *and* for k values near the peak of the structure factor; furthermore, the mode-coupling amplitudes are much larger near the peak of the structure factor so that the contributions at these large k values actually yield the dominant slowly decaying component.

To calculate the amplitudes, the two-particle direct correlation function is determined from the Percus-Yevick equation, with Verlet-Weiss corrections [15]. The longitudinal amplitude for Γ depends also on the three-point correlation function. Most previous calculations have either neglected this term (convolution approximation) or used the superposition approximation. Both of these approximations are known to be poor over wide ranges of k values. To explore the relative importance of this term we compare these approximations to a more accurate form recently proposed by Curtain and Ashcroft [19]. Figure 3(a) shows that the superposition and convolution approximations for $\mathcal{A}_2$ are very poor for $x<0.2$ (below the peak of the structure factor), while they are better approximations for $x>0.2$. Figure 3(b) shows that the factor $\mathcal{B}(x)$ from the correlation functions has a sharp peak near $x=0.2$. This is due to the soft-heat mode. The composition of $\mathcal{A}_2$ and $\mathcal{B}$ is shown in Fig. 3(c), showing that the domain of large differences below $x=0.2$ is not relevant for the integrals. Differences of the order of 100% still occur in a narrow range near the peak of the structure factor; however, the resulting differences in the transport coefficients is only of the order of 1%. It is possible that such differences become more important at larger k values, so all calculations below are performed using the Curtain-Ashcroft three-particle correlation function.

With the amplitudes known the viscosities can be calculated from (4.4). Figure 4 shows the kinematic viscosity relative to its Enskog value, ν/ν_0, as a function of the density [$\nu_0\equiv\nu(k=0)$]. There is a strong enhancement in the vicinity of freezing for both coefficients, due to the monotonic softening of the heat mode at large wave vectors. Also shown for comparison are some results from computer simulation [20]. Two values of the crossover time to mode coupling, τ in Eq. (3.10), are shown. The value $\tau=10t_E$ was chosen in Ref. [11] for the best fit to computer simulation for the stress tensor time correlation function; it is seen to be consistent with the viscosity data as well. The graph of Γ/Γ_0 is indistinguishable from Fig. 4 and is not shown (this near equivalence is due to the fact that the mode-coupling effects on the longitudinal damping constant occur only through enhancement of the shear viscosity). Clearly, the mode-coupling effects on renormalizing Navier-Stokes transport coefficients become significant at high densities. This suggests that other mode-coupling effects on the dispersion relations at larger wave vectors are also significant, as demonstrated in the next section.

V. LARGE-k DISPERSION RELATIONS

The dispersion relations for larger values of k require more detailed evaluation of the mode-coupling integrals as a function of both k and z. Attention is focused on the longitudinal modes which contribute to the density autocorrelation function. The dispersion relations are obtained from Eq. (2.10) with $M(k,z)$ restricted to the three-dimensional longitudinal subspace. Equivalently, we can look directly at the spectrum of the (normalized) density autocorrelation function,

$$\tilde{F}(k,z)\equiv\tilde{C}_{pp}(k,z)/C_{pp}(k,0)\ . \tag{5.1}$$

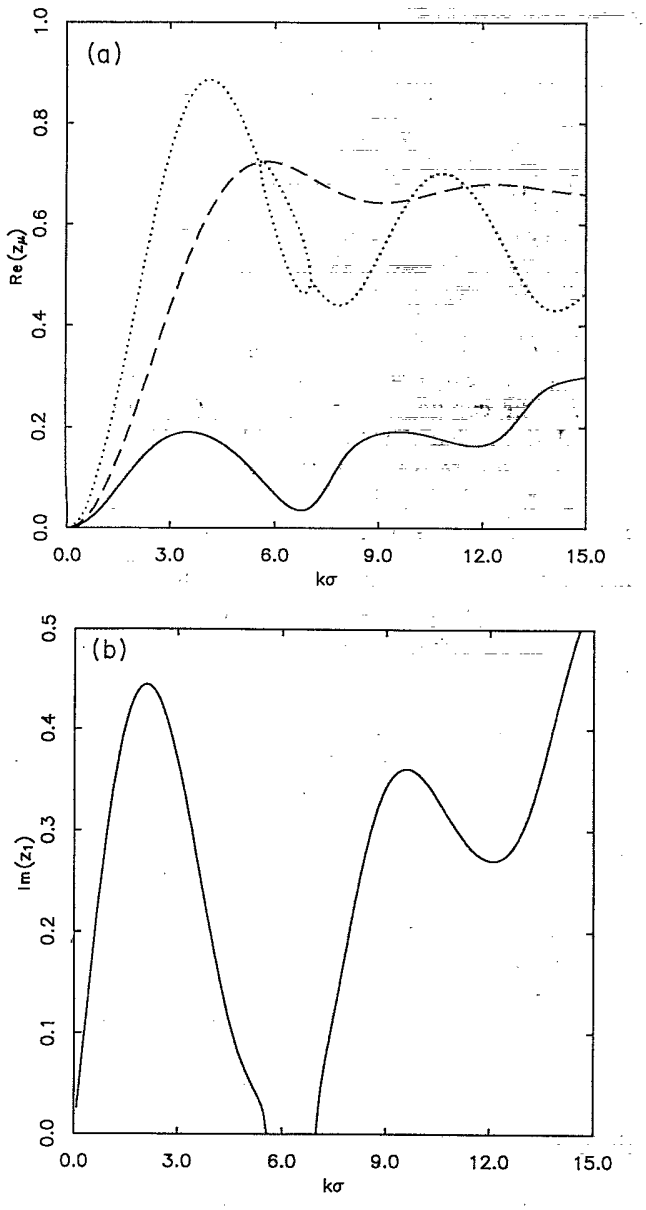

FIG. 1. (a) Real part of $-z_\mu(k)=\lambda_\mu(k)$, obtained by neglecting mode-coupling effects: heat mode (——), sound modes (· · ·), and shear modes (— — —), all at $n^*=0.9$. (b) Imaginary part of sound modes, calculated as in (a).

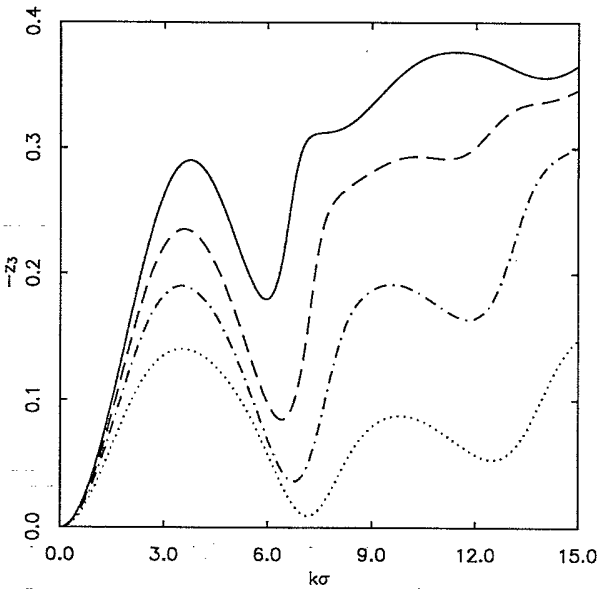

FIG. 2. Softening of the heat mode as a function of the density, calculated as in Fig. 1 at $n^*=0.7$(——), $n^*=0.8$(— — —), $n^*=0.9$–·–·–), and $n^*=1.04$(· · ·).

This can be expressed in a suggestive viscoelastic form (see Appendix),

$$\tilde{F}(x,z)=[z+k^2\gamma(k,z)][z^2+zk^2\gamma(k,z)+\Omega^2(k)k^2]^{-1}\ , \tag{5.2}$$

where $\gamma(k,z)$ and $\Omega(k)$ are defined in terms of the transport matrix, M, by

$$k^2\gamma(k,z)\equiv M_{33}(k,z)-M_{32}(k)[z+M_{22}(k)]^{-1}M_{23}(k)\ , \tag{5.3}$$

$$\Omega^2(k)k^2=-M_{31}(k)M_{13}(k)=k^2/\beta mnS(k)\ . \tag{5.4}$$

If $\gamma(k,z)$ and $\Omega(k)$ were constants, (5.2) would describe two sound modes with damping constant γ and speed Ω. Consequently, effects of the finite wave vector and other excitations are completely contained in these two quantities. In the approximation $M(k,z)\to M(k)$, the additional z dependence of $\gamma(k,z)$ is due to the matrix elements M_{23} and M_{32}, relating the momentum density to energy density fluctuations. The resulting $\tilde{F}(k,z)$ then contains the heat mode as well as the two sound modes.

The soft-heat mode at high density near the peak of the structure factor can be understood qualitatively from the form (5.2) as follows. Since $S(k)$ has a large maximum, $\Omega(k)$ is small in the vicinity of that maximum; in addition, at high density the viscosity, and hence γ, is large. The dispersion relations for (5.2) are then approximately determined from

$$z_3+\Omega^2(k)/\gamma(k,z_3)=0\ . \tag{5.5}$$

Assuming that the solution to (5.5) near $k=k_0$ is small enough to replace $\gamma(k,z)\to\gamma(k,0)$, the result becomes simply $z\sim\Omega^2(k)/\gamma(k,0)$ which is in reasonable agreement with the heat mode shown in Fig. 2 near its

minimum.

More generally, the complete longitudinal dispersion relations are obtained from solutions to

$$z^2+zk^2\gamma(k,z)+\Omega^2(k)k^2=0\ . \tag{5.6}$$

It is tempting to solve this equation by iterating around the Enskog solutions. First, however, it is necessary to investigate the analytic continuation of the mode-coupling integrals to the $z<0$ half plane. Use of (4.2) in (3.10) gives the relevant mode-coupling integral as a function of z and k,

$$\Gamma^{\mathrm{MC}}(k,z)k^2=\sum_{\mu=1}^{3}\sum_{\mu'=1}^{3}\int d\mathbf{k}'\ A_2(\mathbf{k}',\mathbf{k}-\mathbf{k}')R_\mu(\mathbf{k}')R_{\mu'}(\mathbf{k}-\mathbf{k}')$$
$$\times[z+\lambda_\mu(k')+\lambda_{\mu'}(|\mathbf{k}-\mathbf{k}'|)]^{-1}\exp\{-[z+\lambda_\mu(k')+\lambda_{\mu'}(|\mathbf{k}-\mathbf{k}'|)]\tau\}\ . \tag{5.7}$$

In practice, it is found that only the heat modes ($\mu=\mu'=3$) have a significant contribution to the k' integral in (5.7),

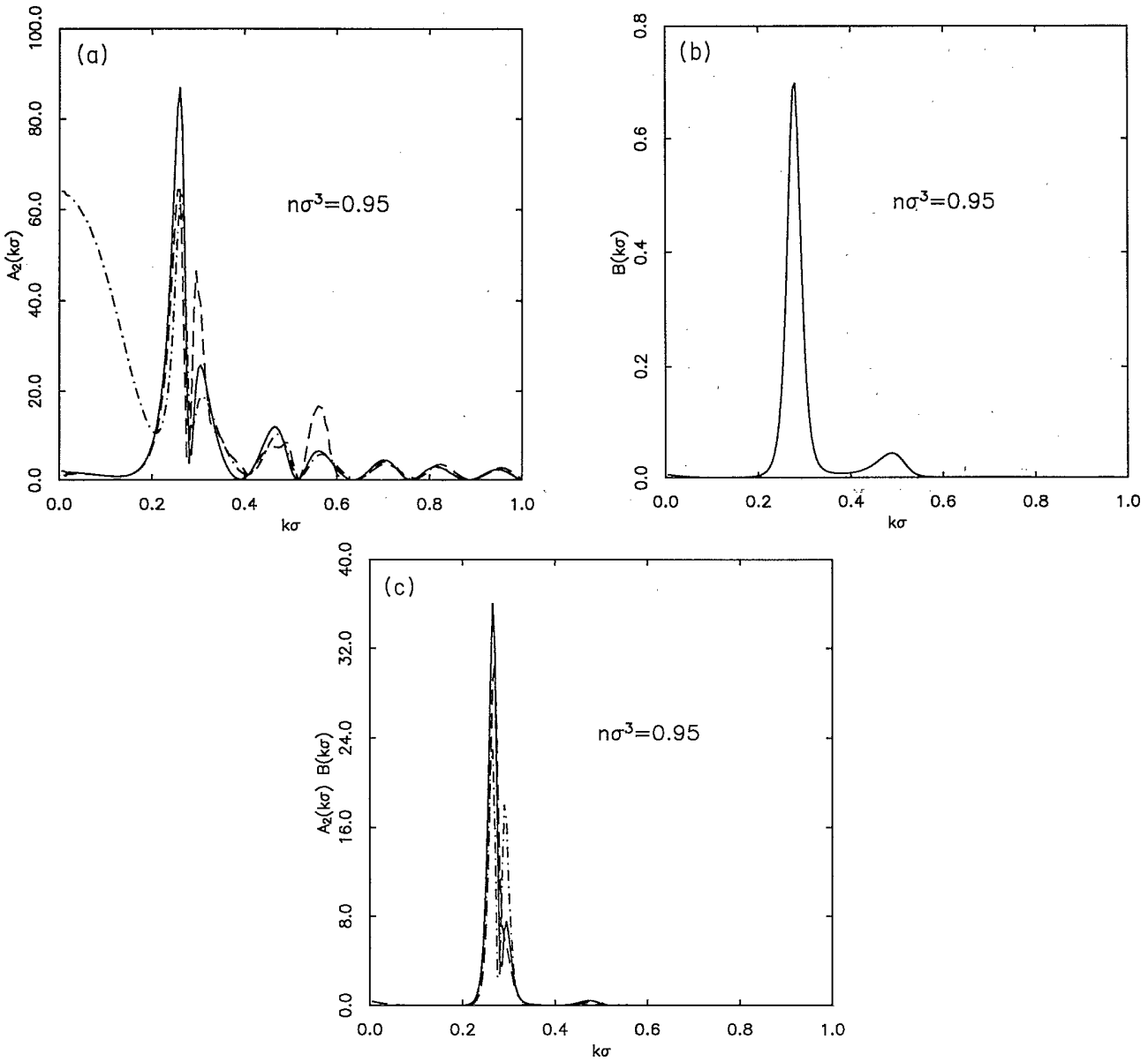

FIG. 3. (a) Mode-coupling amplitudes, $\mathcal{A}_2(k\sigma)$, from Eq. (4.5) at $n^*=0.95$. (b) Mode-coupling amplitude, $\mathcal{B}(k\sigma)$, from Eq. (4.5) at $n^*=0.95$. (c) Mode-coupling amplitude, $\mathcal{A}_2(k\sigma)\mathcal{B}(k,\sigma)$, from Eq. (4.5) at $n^*=0.95$.

over the k range of interest ($k<25\sigma^{-1}$), with differences of only a few percent due to inclusion of the sound modes. To simplify the discussion of analyticity (5.7) is replaced by the simpler dominant part [numerical calculations, however, use the more general form (5.7)],

$$\Gamma^{\mathrm{MC}}(k,z)k^2=e^{-z\tau}\int d\mathbf{k}'\,G(\mathbf{k}',\mathbf{k},z)[z+\lambda_3(k')+\lambda_3(|\mathbf{k}-\mathbf{k}'|)]^{-1}\,, \tag{5.8}$$

$$G(\mathbf{k}',\mathbf{k},z)\equiv A_2(\mathbf{k}',\mathbf{k}-\mathbf{k}')R_3(\mathbf{k}')R_3(\mathbf{k}-\mathbf{k}')\exp\{-[z+\lambda_\mu(k')+\lambda_{\mu'}(|\mathbf{k}-\mathbf{k}'|)]\tau\}. \tag{5.9}$$

The function, $\lambda_3(k)$, is real and positive for all k so $\Gamma^{\mathrm{MC}}(k,z)$ is analytic in the half plane, $\mathrm{Re}\,z>0$. However, solutions to (5.6) are expected in the vicinity of $z\sim-\lambda_3(k)$ so it is necessary to analytically continue the integral representation to $z\le 0$. The integrand of (5.8) has its first singularity along the real axis at $z=-z_{\min}(k)\equiv\min\{\lambda_3(k')+\lambda_3(|\mathbf{k}-\mathbf{k}'|)\}$, the minimum with respect to all k' and $\hat{\mathbf{k}}\cdot\hat{\mathbf{k}}'$ for fixed $\mathbf{k}$. Figure 5 shows $z_{\min}(k)$ at $n^*=0.9$, together with $\lambda_3(k)$ for comparison. The result can be understood as follows. For small k, $z_{\min}(k)\sim\{\lambda_3(0)+\lambda_3(|\mathbf{k}-\mathbf{0}|)\}=\lambda_3(k)$; similarly, near the peak of the structure factor, $k=k_0$, the minimum occurs for $z_{\min}\sim\{\lambda_3(k_0)+\lambda_3(|\mathbf{k}_0-\mathbf{k}_0|)\}=\lambda_3(k_0)$. In the vicinity of k_0 and for small k, $z_{\min}(k)$ remains similar to $\lambda_3(k)$. However, at $k\sigma\sim 2$ it saturates at a value

$$z_{\min}(k)\sim\{\lambda_3(k_0)+\lambda_3(|\mathbf{k}-\mathbf{k}'|=k_0)\}=2\lambda_3(k_0)\,.$$

If the singularity of the integrand at $z=-z_{\min}(k)$ is integrable and $\Gamma^{\mathrm{MC}}(k,z)$ is smooth in the vicinity then $\Gamma^{\mathrm{MC}}(k,z)$ remains analytic up through this point; otherwise, $-z_{\min}(k)$ represents a branch point on the real axis. In the latter case, we choose the branch line to extend along the real axis from $-z_{\min}$ to $-\infty$ and define $\Gamma^{\mathrm{MC}}(k,z)$ to be the analytic continuation to the domain $-\pi<\theta<\pi$, where θ is the phase angle for $z+z_{\min}\equiv Re^{i\theta}$. Numerical evaluation at $n^*=0.9$ provides the following typical results. For $k\sigma<1.8$ and for $k\sigma>5.2$, $\Gamma^{\mathrm{MC}}(k,z)$ is finite and smooth near $z=-z_{\min}(k)$. However, for $1.8<k\sigma<5.2$, $z=-z_{\min}(k)$ represents a branch point. Figure 6 illustrates these two cases, showing $\Gamma^{\mathrm{MC}}(k,z)$ as a function of real z for $k\sigma=1.5$, 2.0, and 6.8.

This analysis of the analytic continuation shows there can be no real solution to the dispersion relations (5.6) for $z<-z_{\min}(k)$ for $1.8<k\sigma<5.2$. Since $\lambda_3(k)>z_{\min}(k)$ in this range, an iterative or perturbative solution about $\lambda_3(k)$ is not possible. Instead, for each k numerical solutions to (5.6) have been attempted in the portion of the z plane for which $\Gamma^{\mathrm{MC}}(k,z)$ is well defined. The results are shown in Fig. 7, along with $\lambda_3(k)$ and $z_{\min}(k)$ for comparison. The lower curve is a real solution for all k, which is similar to $\lambda_3(k)$ for small k and for k near k_0. In the intermediate-k range it follows closely $z_{\min}(k)$ but always lies below that value, as required by analyticity of $\Gamma^{\mathrm{MC}}(k,z)$. The upper curve in this figure is the real part of a pair of complex conjugate solutions, whose imaginary part is shown in Fig. 8. It is likely that this is a remnant of the extended sound modes, although significantly modified in the intermediate-k range by the branch cut. The gap in the imaginary part also appears at approxi-

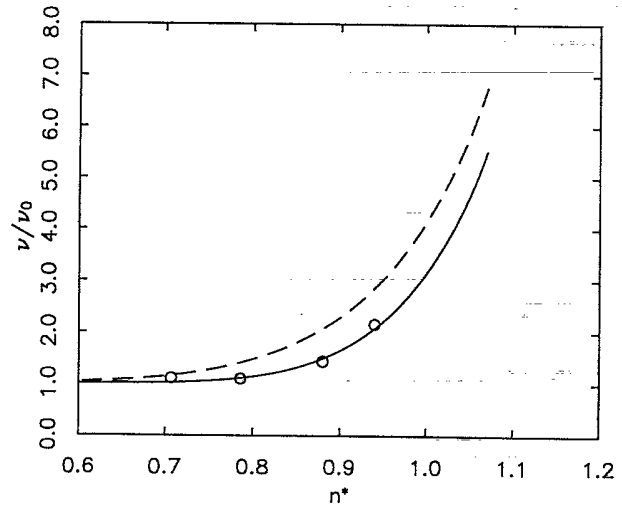

FIG. 4. Kinematic viscosity, ν, relative to its value neglecting mode-coupling effects, ν_0, as a function of density using $\tau=10$ (——) and $\tau=5$ (— — —). Circles denote computer simulation results from Ref. [20].

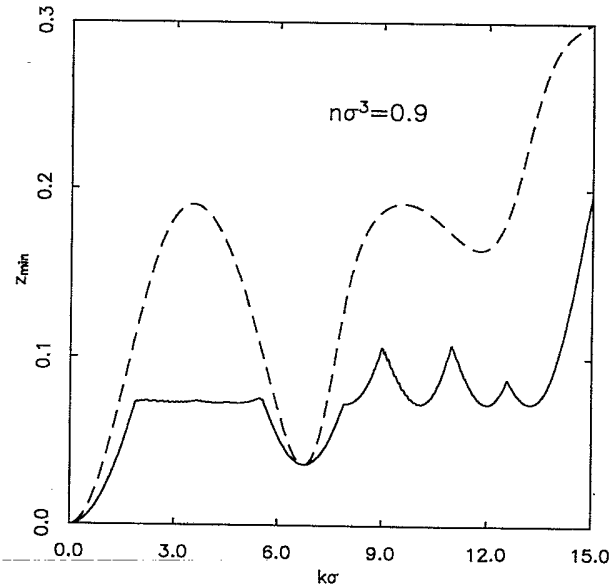

FIG. 5. Magnitude of singularity in the mode-coupling integral, (5.8), $\min\{\lambda_3(k')+\lambda_3(|\mathbf{k}-\mathbf{k}'|)\}$ as a function of $k\sigma$ at $n^*=0.9$. Also shown for comparison is $\lambda_3(k)$ (· · ·).

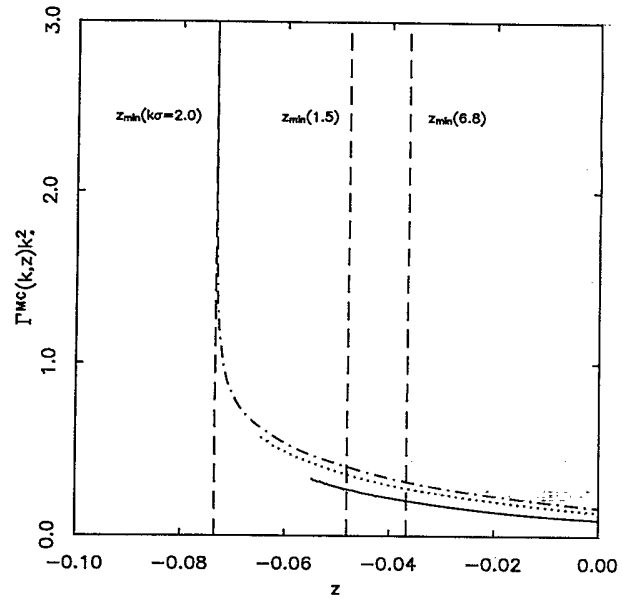

FIG. 6. Mode-coupling integral, (5.7), as a function of z near z_{min} for $k\sigma=6.8$ (——), $k\sigma=2.0$ (–·–·), and $k\sigma=1.5$ (· · ·), all at $n^*=0.9$.

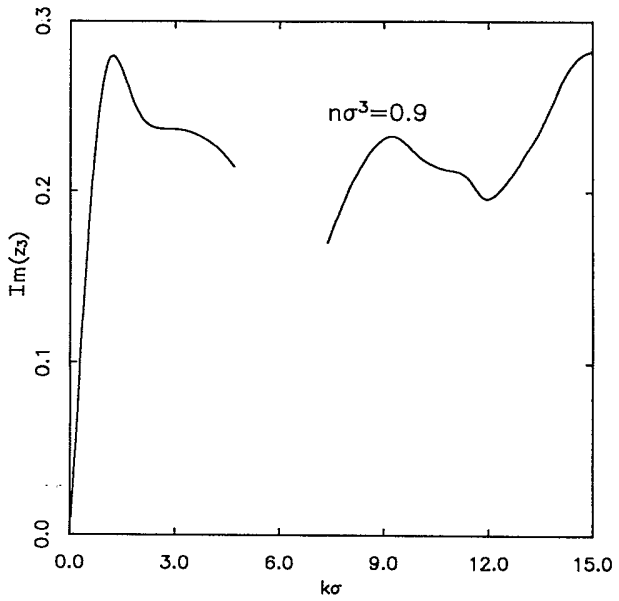

FIG. 8. Same as Fig. 7 for the imaginary part.

mately the same k values as in the Enskog case, although no corresponding new solutions are now found in the gap. The latter are prohibited above $z_{min}(k)$ due to the analyticity conditions on $\Gamma^{MC}(k,z)$. In the following, the lower real curve will be referred to as the modified heat mode, $z_h(k)$, and the additional complex solutions as the modified sound modes, $z_\pm(k)$.

In summary, the sound and heat mode branches still exist when mode-coupling effects are important. Quantitative differences are most significant at intermediate-k values for which there is a branch point. The heat mode for k values near the peak of the structure factor is further softened by the mode-coupling effects. In the next section, it is shown that the heat mode in this region is a simple pole of the density autocorrelation function whose residue is close to one. Consequently, it describes the dominant time dependence of this correlation function.

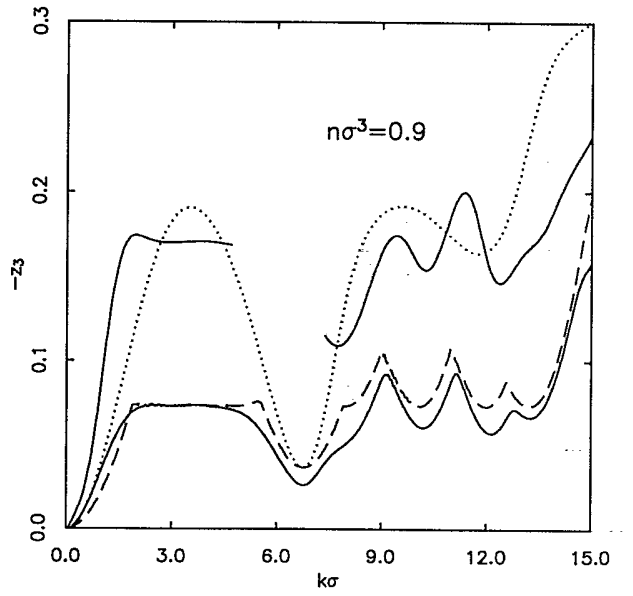

FIG. 7. Real part of dispersion relations from Eq. (5.6) at $n^*=0.9$. Solid curves denote solutions to this equation as a function of $k\sigma$; also shown are $\lambda_3(k\sigma)$ (· · ·), and the magnitude of $z_{min}(k\sigma)$ (— — —), for comparison.

VI. DENSITY AUTOCORRELATION FUNCTION

The time dependence of the correlation functions is determined from their analytic structure, according to (2.8). The dispersion relations of the last section determine the singular points, but not the nature of the singularity. Additional time dependence is generated from deformation of the contour around any branch cuts. To determine the relative importance of contributions from the dispersion relations of Sec. V the density autocorrelation function, $\tilde{F}(k,z)$, defined in (5.1) is calculated numerically and then represented as

$$\tilde{F}(k,z)=A(k)[z+z_\mu(k)]^{-\alpha(k)}+\Delta\tilde{F}(k,z)\ . \qquad (6.1)$$

Here $\Delta\tilde{F}(k,z)$ is the regular part of $\tilde{F}(k,z)$ at $z=-z_\mu(k)$. The amplitude, $A(k)$, and exponent, $\alpha(k)$, are determined by evaluation of $\tilde{F}(k,z)$ in the vicinity of $-z_\mu(k)$, and the results are shown in Fig. 9 using $z_\mu=z_3$ (again for $n^*=0.9$). Near k_0 the exponent $\alpha(k)=1$, so the heat mode is a simple pole. Furthermore, the amplitude is ~ 0.9 so this heat mode is the dominant contribution to the density autocorrelation function. At larger- and smaller-k values the amplitude is much smaller, and the other singularities have significant contributions. The fitting in this range becomes more difficult, as the relative contributions from $\Delta\tilde{F}(k,z)$ are small only for much smaller $|z+z_h(k)|$. Qualitatively, it appears that for $0.5<k<5$ the exponent deviates from one, indicating

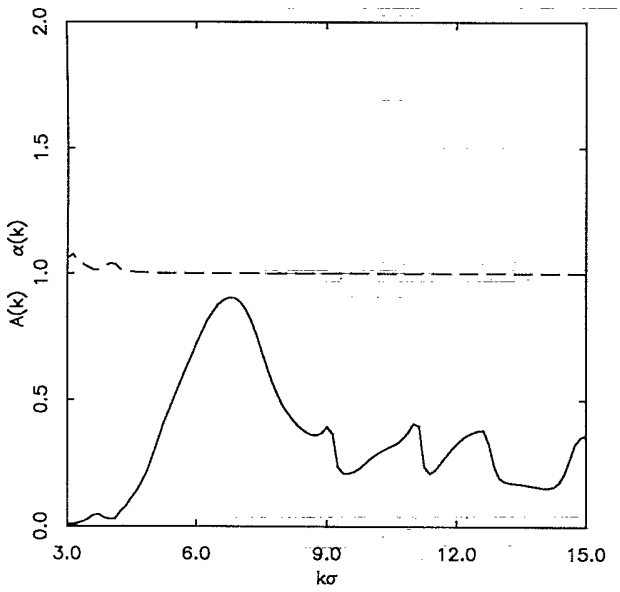

FIG. 9. Amplitude $A(k)$ (——), and exponent $\alpha(k)$ (— — —) of $z_3(k)$ singularity in Eq. (6.1) at $n^*=0.9$.

that the heat mode represents a branch point rather than a simple pole.

Inverting the Laplace transform of (6.1) for k near k_0 gives

$$F(k,t)=A(k)e^{z_h(k)t}+\Delta F(k,t)\ . \tag{6.2}$$

To calculate the complete $F(k,t)$, Eq. (5.2) is first converted to the equivalent real-time integro-differential equation by inverting the Laplace transform of

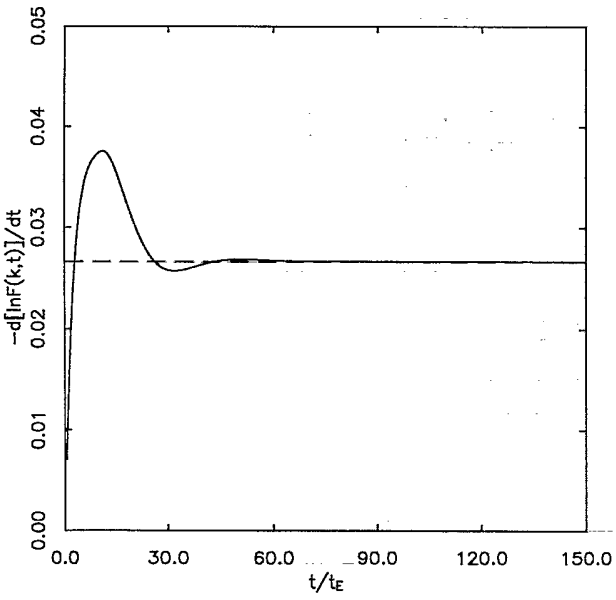

FIG. 10. Time derivative of $\ln F(k,t)$ as a function of time relative to the Enskog mean free time, t_e, at $n^*=0.9$ and $k=k_0$.

$$[z^2+zk^2\gamma(k,z)+\Omega^2(k)k^2]\tilde{F}(k,z)=z+k^2\gamma(k,z) \tag{6.3}$$

to get the second-order ordinary differential equation,

$$\left[\frac{\partial^2}{\partial t^2}+\Omega^2(k)\right]F(k,t) + k^2\int_0^\infty d\tau\,\gamma(k,t-\tau)\frac{\partial}{\partial\tau}F(k,\tau)=0\ . \tag{6.4}$$

The solution to this equation gives the exact result for our model. It is more convenient for calculations than the Laplace representation when no distinction between contributions from the hydrodynamic poles and other parts of the spectrum is desired. The method used for numerical solution is described elsewhere [21]. Figure 10 shows a comparison of the exact solution with the contribution from the heat mode only [first term on the right side of (6.2)] for $k=k_0$ and $n^*=0.9$. For long times, $t>75t_e$, the time dependence is governed by the heat mode and contributions from *all* other singularities (poles and branch cuts) have decayed to negligible relative values.

VII. DISCUSSION

The objective here has been a qualitative study of hydrodynamic modes in dense fluids over a wide range of wave vectors. The analysis extends that of Cohen and de Schepper, based on the Enskog kinetic theory, to include lowest-order mode-coupling effects. We first make some remarks regarding the model used here to study the following problems.

(1) There are many quantitative uncertainties associated with current mode-coupling models, particularly regarding intermediate time behavior. Here we have tried to make them explicit to emphasize the qualitative nature of information available about dense fluids. For example, the value of τ chosen to represent the time after which mode-coupling effects dominate was not calculated, but rather determined from a fit to computer simulation data for the stress-tensor autocorrelation function.

(2) The time dependence predicted by the model for $t<\tau$ is certainly not correct. In fact, it neglects entirely the microscopic modes that relax on the time scale of the mean free time. However, these time scales are not important for the questions raised here regarding hydrodynamics.

(3) In general, the mode-coupling amplitudes depend on three-particle correlations which are significantly different from those frequently calculated in the superposition or convolution approximations at wave vectors below the peak of the structure factor [Fig. 3(a)]. However, the hydrodynamic mode-coupling contributions are highly localized about the peak of the structure factor so that the three-particle correlations are not important for the viscosities [Fig. 3(c)]. For similar reasons the coupling of sound modes is also negligible. These observations justify the simplifications made in most previous calculations.

(4) The mode-coupling renormalization of transport coefficients leads to significant enhancement of the

viscosities for $n^* > 0.7$, in agreement with computer-simulation results. However, the good agreement shown in Fig. 4 is fortuitous as the results are sensitive to the value of τ chosen.

We now summarize and comment on the nature of the hydrodynamic modes when both mode-coupling and finite wave-vector effects are important.

(1) For asymptotically small wave vectors the hydrodynamic modes have the form associated with the Navier-Stokes equations; however, there is a branch point and associated cut due to mode-coupling effects that lead to competing dynamics on the same time scale.

(2) The Navier-Stokes hydrodynamic modes extend to branches that exist for wave vectors of the order of the inverse correlation length. Neglecting mode-coupling effects, the heat mode is seen to soften for wave vectors near the peak of the structure factor (Fig. 2) as the density increases. There has been speculation that extrapolation of this trend to metastable densities leads to a vanishing heat mode, reflecting a mechanical instability [12]. It is this soft-heat mode contribution to the mode-coupling integrals that is responsible for the viscosity enhancement. The dispersion relations obtained from the model including mode-coupling effects show a further softening of the heat mode.

(3) The singularity of the mode-coupling integrand has a k dependence shown in Fig. 5. For intermediate-k values, this singularity is not integrable and leads to a branch point. This effectively changes the heat mode to a propagating mode, except for k near k_0. Additional complex branch points associated with the sound modes are expected, but were not explored.

(4) The relative contribution of different modes and branch points to the time dependence of the time correlation functions is difficult to assess in general, since the nature of the singularities is not known. However, for k near k_0, it is found that the soft heat mode is a simple pole and its contribution completely dominates the long-time dependence of the density autocorrelation function.

Finally, we remark on the relationship to mode-coupling models of the "ideal" glass transition. The simplest model of this type is obtained by using the exact correlation functions on the right sides of (3.7) and (3.10), rather than their Enskog values as done here. The correlation functions are then determined self-consistently from (3.7), (3.10), and (2.9). Improvement to include self-consistency for the dense equilibrium fluid [10] ($n^* < 0.9$) is not yet justified in our view since the uncertainties associated with intermediate-time dynamics and corresponding crossover time to mode coupling compromise any claims to quantitative accuracy (recall Fig. 4). For higher densities (metastable fluid states) these uncertainties in the crossover time become less important as the mode-coupling integral grows without bound; the viscosity enhancement of Fig. 4 is ultimately divergent, indicating the ideal glass transition [22,23]. However, this divergence is most likely an artifact of the model and the self-consistent mode-coupling approximation is questionable near the divergence as well. More complex versions of self-consistent mode-coupling models that are free of this divergence have been suggested for the high-density domain [24–26] though their basis is more phenomenological and they have not been explored quantitatively. We emphasize that the extensive studies of analytic properties of the density autocorrelation function near the ideal glass transition are quite different in objective than those presented here. In particular, they make no attempt to determine a relationship of the ideal glass transition to hydrodynamic modes.

ACKNOWLEDGMENTS

This research was supported in part by National Science Foundation Grant No. INT 8712576 and by the Division of Sponsored Research at the University of Florida. S.P.D. is also grateful to the International Center for Theoretical Physics at Trieste, for their hospitality. S.P.D. was supported in part by the Stichting voor Fundamental Onderzoek der Materie (FOM), which is sponsored by de Nederlandse Organistie voor Wetenschappelijk Onderzoek (NWO).

APPENDIX: DETAILS OF THE MODEL

The representation (2.9) follows directly from the Liouville equation by the Zwanzig-Mori projection operator method, with some modifications for the singular hard-sphere interactions [27]. Define a projection operator onto the set of conserved densities defined in Eq. (2.2) as

$$PX = \langle X \rangle + \langle X[a_\alpha - \langle a_\alpha \rangle]^* \rangle g^{-1}_{\alpha\beta}[a_\beta - \langle a_\beta \rangle] ,$$
$$g_{\alpha\beta} = \langle a_\alpha [a_\beta - \langle a_\beta \rangle] \rangle . \quad \text{(A1)}$$

Then it is found that the matrix $M(k,z)$ for the correlation functions is given exactly by

$$M(k,z) = M(k,\infty) + \Delta M(k,z) , \quad \text{(A2)}$$

$$M_{\alpha\beta}(k,\infty) = -\langle [L_+ a_\alpha][a_\gamma - \langle a_\gamma \rangle] \rangle g^{-1}_{\gamma\beta} , \quad \text{(A3)}$$

$$\Delta M_{\alpha\beta}(k,z) = \int_0^\infty dt\, e^{-zt} \langle [e^{L't} Q L_+ a_\alpha][Q L_- a_\gamma] \rangle g^{-1}_{\gamma\beta} . \quad \text{(A4)}$$

Here, $Q = 1 - P$ is the projection orthogonal to the linear subspace of conserved densities, and $L' = QL_+Q$ is the generator for dynamics in this orthogonal subspace. The operators L_+ and L_- denote the hard-sphere Liouville operators for forward and backward streaming, respectively [27]. Note that $L_\pm \sim a_\alpha$ as a consequence of the $\{a_\alpha\}$ being local conserved densities. Consequently, $M_{\alpha\beta}(k,\infty)$ is of order k, and $\Delta M_{\alpha\beta}(k,z)$ is of order k^2. This justifies the form (2.12).

The matrix g is diagonal with elements

$$g_{11} = mn^2 S(k),\ g_{22} = 3n/2\beta^2 ,$$
$$g_{33} = g_{44} = g_{55} = nm/\beta \quad \text{(A5)}$$

where n is the density and $\beta = (k_B T)^{-1}$. The matrix elements of $M(k, z=\infty)$ have been evaluated elsewhere [27]. The nonzero elements in dimensionless form are

$$\begin{aligned}
&\overline{M}_{\alpha\beta}=t_e h_\alpha^{-1} M(k,z=\infty)h_\beta \ \text{ (no sum on } \alpha,\beta), \quad h_\alpha=(m,\beta^{-1},\sqrt{m/\beta},\sqrt{m/\beta},\sqrt{m/\beta}) , \\
&\overline{M}_{13}=-ix\sqrt{\pi}/6y, \quad \overline{M}_{31}=\overline{M}_{13}/S(k), \quad \overline{M}_{22}=\tfrac{2}{3}[1-j_0(x)] , \\
&\overline{M}_{23}=\overline{M}_{13}[1+3yj_1(x)/x], \quad \overline{M}_{32}=\tfrac{2}{3}\overline{M}_{23} , \\
&\overline{M}_{33}=\tfrac{2}{3}[1-3j_0(x)+6j_1(x)/x], \quad \overline{M}_{44}=\overline{M}_{55}=\tfrac{2}{3}[1-3j_1(x)/x] ,
\end{aligned} \tag{A6}$$

where $j_n(x)$ is the nth-order spherical Bessel function, $S(k)$ is the static structure factor, $x=k\sigma$, $t_e=\sigma\sqrt{\beta m\pi}/6y$, and $y=2\pi n^* g(\sigma)/3$.

Consider next the evaluation of $\Delta M(k,z)$. The operators L_+ and L_- operating on the mass density, a_1, yield ka_3 as a consequence of the microscopic continuity equation. Consequently, $\Delta M_{\alpha 1}=\Delta M_{1\alpha}=0$ for all α. Also, parity considerations and rotational invariance lead to the fact that ΔM is block diagonal of the form

$$\Delta M=\begin{bmatrix} 0 & 0 & 0 & 0 & 0 \\ 0 & \Delta M_{22} & \Delta M_{23} & 0 & 0 \\ 0 & \Delta M_{32} & \Delta M_{33} & 0 & 0 \\ 0 & 0 & 0 & \Delta M_{44} & 0 \\ 0 & 0 & 0 & 0 & \Delta M_{55} \end{bmatrix} . \tag{A7}$$

Furthermore, $\Delta M_{44}=\Delta M_{55}$.

The hydrodynamic poles (longitudinal modes) are obtained from the dispersion relations $\mathrm{Det}[z_\mu+M]=0$, or

$$z_\mu^2+z_\mu k^2\gamma(k,z_\mu)+\Omega^2(k)k^2=0, \quad \mu=1,2,3 , \tag{A8}$$

$$z_4+M_{44}(k,z_4)=0 , \tag{A9}$$

and $z_5=z_4$. In (A8) $\gamma(k,z)$ and $\Omega(k)$ are given by

$$\begin{aligned}
k^2\gamma(k,z)\equiv& M_{33}(k,z) \\
&-M_{32}(k,z)[z+M_{22}(k,z)]^{-1}M_{23}(k,z),
\end{aligned} \tag{A10}$$

$$\Omega^2(k)k^2\equiv -M_{31}(k,\infty)M_{13}(k,\infty)=k^2/\beta mnS(k) . \tag{A11}$$

The correlation function can then be expressed as

$$\begin{aligned}
&\tilde{F}(k,z)=[z+\Sigma(k,z)]^{-1} , \\
&\Sigma(k,z)=\Omega^2(k)k^2/[z+\gamma(k,z)] .
\end{aligned} \tag{A12}$$

As described in Sec. III, only the lowest-order bilinear density mode-coupling contributions to ΔM are retained. In this approximation $\Delta M_{23}=0=\Delta M_{32}$. A detailed evaluation of these elements leads to the results given by Eqs. (3.7) and (3.10).

To calculate the mode-coupling integrals, it is necessary to have $\tilde{F}$ calculated with ΔM neglected, (4.2). The eigenvalues, $\lambda_\mu(k)=-z_\mu$, and associated eigenvectors are calculated from (A8) and (A9) with $M(k,z)\to M(k,\infty)$. Equation (A8) then becomes a cubic equation determining the two sound modes and the heat mode, Eq. (A9) gives directly the twofold-degenerate shear mode. The residues are then determined from (A12),

$$\begin{aligned}
R^\mu(k)&=\left[1+\frac{d}{dz}\Sigma(k,z)\bigg|_{z=z_\mu}\right]^{-1} \\
&=1-\left[\frac{z_\mu}{\Omega}\right]^2\left[1+\frac{M_{23}M_{32}}{(z_\mu+M_{22})^2}\right]^{-1} .
\end{aligned} \tag{A13}$$

[1] J. A. McLennan, *Introduction to Nonequilibrium Statistical Mechanics* (Prentice-Hall, Englewood Cliffs, NJ, 1989).
[2] L. Onsager, Phys. Rev. **37**, 405 (1931); **38**, 2265 (1931).
[3] L. P. Kadanoff and P. C. Martin, Ann. Phys. (N.Y.) **24**, 419 (1963).
[4] J. A. McLennan, Helv. Phys. Acta **40**, 645 (1967); J. Dufty and J. A. McLennan, Phys. Rev. **172**, 176 (1968); J. Dufty, *ibid.* **176**, 398 (1968).
[5] I. de Schepper and E. Cohen, J. Stat. Phys. **27**, 223 (1982).
[6] For early references, see T. Keyes, in *Statistical Mechanics*, edited by B. Berne (Plenum, New York, 1977), Pt. B.
[7] M. G. Ernst and J. R. Dorfman, Physica **61**, 157 (1972); J. Stat. Phys. **12**, 311 (1975).
[8] J. W. Dufty, Phys. Rev. **5**, 2247 (1972).
[9] E. G. D. Cohen, I. M. de Schepper, and M. Zuilhof, Physica B **127**, 282 (1984).
[10] E. Leutheusser, J. Phys. C **15**, 2801 (1982); **15**, 2827 (1982).
[11] T. Kirkpatrick, Phys. Rev. Lett. **53**, 1735 (1984); **53**, 2185 (1984); T. Kirkpatrick and J. Nieuwoudt, Phys. Rev. A **33**, 2651 (1986).
[12] I. de Schepper, A. F. E. Haffmans, and H. van Beijeren, Phys. Rev. Lett. **57**, 1715 (1986).
[13] J. A. McLennan, Phys. Fluids **9**, 1581 (1966).
[14] M. C. Marchetti, G. Garland, and J. Dufty, Phys. Rev. A **25**, 1218 (1982).
[15] J-P. Hansen and I. McDonald, *Theory of Simple Liquids* (Academic, New York, 1976).
[16] B. Berne, in *Statistical Mechanics* (Ref. [6]).
[17] T. Kirkpatrick, Phys. Rev. A **32**, 3130 (1985).
[18] J. A. Leegwater and H. van Beijeren, J. Stat. Phys. **57**, 383 (1989); J. A. Leegwater, J. Chem. Phys. **92**, 4394 (1990).
[19] W. Curtain and N. Ashcroft, Phys. Rev. Lett. **53**, 2385 (1987).
[20] B. Alder, D. Gass, and T. Wainwright, J. Chem. Phys. **53**, 3813 (1970); J. P. J. Michels and N. Trappeniers, Physica A **104**, 243 (1980).

[21] S. P. Das, Phys. Rev. A **42**, 6116 (1990).
[22] E. Leutheusser, Phys. Rev. A **29**, 2765 (1984); Z. Phys. B **55**, 235 (1984).
[23] U. Bengtzelius, W. Goetze, and A. Sjolander, J. Phys. C **17**, 5915 (1984).
[24] S. P. Das and G. Mazenko, Phys. Rev. A **34**, 2265 (1986).
[25] W. Goetze and L. Sjogren, Z. Phys. B **65**, 415 (1987).
[26] T. Kirkpatrick, Phys. Rev. A **31**, 939 (1985).
[27] J. Lutsko, J. Dufty, and S. P. Das, Phys. Rev. A **39**, 1311 (1989).